Journal of the European Ceramic Society 21 (2001) 941–946

www.elsevier.com/locate/jeurceramsoc

On the local crack resistance of Al_2O_3–TiC composites evaluated by direct indentation method

Jianghong Gong *, Zhe Zhao, Zhenduo Guan

Department of Materials Science and Engineering, Tsinghua University, Beijing 100084, People's Republic of China

Received 27 April 2000; received in revised form 28 August 2000; accepted 10 September 2000

Abstract

Vickers indentation tests were conducted on an Al_2O_3–TiC composite at different load levels. The crack resistance calculated from the length of the indentation-induced crack exhibits a large scatter. Such a large scatter can be characterized well with Weibull statistics and can be attributed to the effect of microstructural inhomogeneity on the local crack resistance. The effect of the statistical variability in the measured crack resistance on *R*-curve evaluation was also discussed and the direct indentation method was suggested to be the most suitable method for the evaluation of the *R*-curve behavior for ceramics.

Keywords: Al_2O_3; Indentation; Mechanical properties; TiC; Toughness and toughening

1. Introduction

The concept of a crack resistance that increases with the length of the crack, i.e. *R*-curve behavior, has been well established for ceramics systems during the past decades.[1–5] The mechanistic origin of *R*-curve behavior has been attributed to the interaction of a propagating crack with inhomogeneities in the microstructure,[6,7] with transformable particles in a process zone,[8,9] and with particles that span the crack.[10,11] Several theoretical models[3,4,12–14] have been proposed to describe the relationship between the *R*-curve behavior and the microstructural characteristics and extensive experimental studies[15–21] have also been conducted to try to develop and standardize the *R*-curve characterization methods for ceramics.

At present, there exist a variety of methods for the *R*-curve characterization. The most commonly used are indentation methods,[15–21] including the direct indentation (DI) method, the indentation–crack-growth (ICG) method and the indentation–strength (IS) method. Some of the conventional fracture mechanics methods, such as the single-edge-notched beam (SENB)[22] and the chevron-notched beam (CNB)[23] methods, have also been employed occasionally. Differences between the *R*-curve characteristics measured with the indentation methods and those measured with the conventional fracture mechanics methods have been generally reported and have been attributed to the fact that the interactions between large cracks and the microstructure are rather different from those between small cracks and the microstructure.[5] However, recent studies[18,19] have shown that the *R*-curve behavior of indentation-induced cracks also depends on the characterization method. For a given material, the *R*-curve measured with the DI method is usually different from those measured with the ICG or the IS methods. To our knowledge, up to now, no satisfactory explanation for these experimental observations has been proposed.

When studying the *R*-curve behavior of a hot-pressed Si_3N_4 ceramic by observing the stable growth of annealed indentation-induced cracks during bending tests, the present authors[24] found that significant deviations exist between the shapes and the locations of the *R*-curves measured with different cracks located in different sites in the specimen surface, making it impossible and unreasonable to fit all the data to a single curve. To explain such an experimental phenomenon, the present authors suggested that the *R*-curve behavior of a given material is dependent not only on the crack length but also on the crack location. In fact, the *R*-curve behavior is already known to be a microstructure-dependent

* Corresponding author. Fax: +86-10-6277-1160.
E-mail address: gong@tsinghua.edu.cn (J. Gong).

0955-2219/01/$ - see front matter
PII: S0955-2219(00)00277-6

phenomenon[1–5] and, when being examined at the microstructural level, any polycrystalline ceramic should be considered to be inhomogeneous. Thus, one can expect that different cracks which are placed in different sites within the material may encounter different variations in crack resistance during extension.

The previous studies concerning the *R*-curve behavior of ceramics have thus far emphasized only the dependence of crack resistance on crack length and have not considered in detail the crack-location dependence of the crack resistance. To ensure the existence of the crack-location dependence of *R*-curve behavior and its effect on the *R*-curve measurement, the direct indentation method was employed in the present study to determine the crack resistance of a TiC particle reinforced Al_2O_3 composite. At each given indentation load level, 30 indentation cracks were introduced in the surface of the test specimen and the statistical variability in the resultant crack resistance data was analyzed.

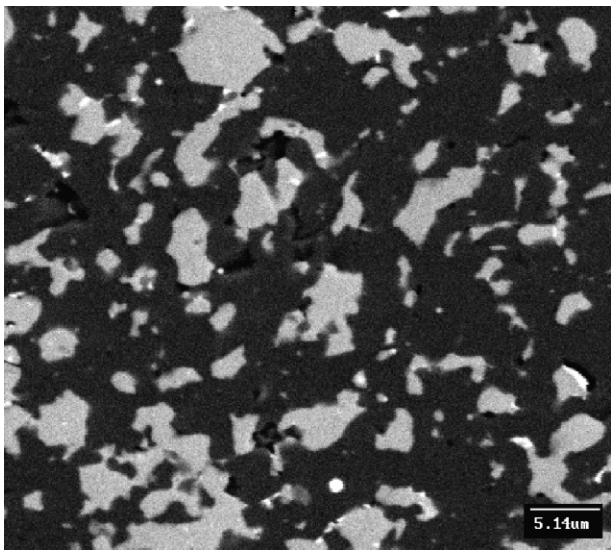

Fig. 1. SEM micrograph showing the polished surface of the test sample. Note that the TiC particles (light phase) were well dispersed in the Al_2O_3 matrix.

2. Experimental

The material selected for the present study was an Al_2O_3 ceramic reinforced with 30 wt.% TiC particles. The basic raw materials used for preparing the composite were a commercial Al_2O_3 powder with an average grain size of 0.5 μm and TiC particles with an average size of 6.8 μm. Both powders were mixed in proper proportion by conventional ball milling with ethyl alcohol and alumina balls in a plastic pot for 4 h. After being dried, the mixed powder was uniaxially pressed at about 40 MPa and then cold isostatically pressed at about 220 MPa to form a disc of about 50 mm diameter. Finally, the disc was hot-pressed at 1650°C and 25 MPa for 30 mm using a graphite die.

A scanning electron microscopy (SEM) micrograph of the polished surface of the hot-pressed product is shown in Fig. 1. As shown, the TiC particles (the light phase) are dispersed uniformly in the Al_2O_3 matrix, but the sizes of the TiC particles exhibit a somewhat large scatter.

The test specimens were directly cut from the hot-pressed product, mounted in bakelite, ground flat and then polished carefully with successively finer diamond pastes to yield a mirror-like surface suitable for indentation. The polished surfaces of the test specimens are perpendicular to the hot-pressing direction. Vickers indentations were made at 49, 98, 196 and 294 N loads on the polished surfaces of the test specimens using a commercial hardness tester (model HV-120, Shandong, China). The indentation crack lengths, $2c_1$ and $2c_2$, as illustrated in Fig. 2, were measured immediately after unloading. A total of 30 perfect indentations, those with clearly symmetrical indentation impressions and with symmetrical crack patterns, were made at each load level. The indentations with clear crack branching were not accepted for the final calculation.

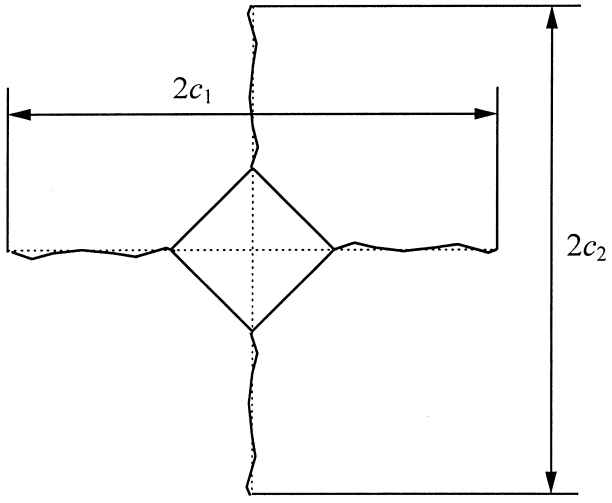

Fig. 2. Characteristic lengths of the cracks introduced by Vickers indentation.

The Knoop indentation method proposed by Marshall et al.[25] was employed to determine the parameter H/E, the ratio of the hardness to the elastic modulus, used for the crack resistance calculation conducted in the following sections. In this method, the parameter H/E is suggested to be related to the long diagonal length, b, and the short diagonal length, a, of the Knoop indentation impression with the following equation[25]

$$\frac{a}{b} = \frac{1}{7.11} - 0.45\left(\frac{H}{E}\right). \quad (1)$$

Five Knoop indentations were made on the polished surface of the test specimen at an indentation load of 33.77 N and the lengths of the long and the short diagonals of each indentation impression were measured. Using the experimental data, the H/E for the present material was determined with Eq. (1) to be 0.0365 with a standard deviation of 0.0034.

3. Calculation of crack resistance

According to the indentation fracture mechanics theory established by Lawn et al.,[26] in the as-indented state, the half-length, c, of a Vickers indentation-induced half-penny surface crack satisfies the following equilibrium relation,[27]

$$K_R = \delta\left(\frac{E}{H}\right)^{1/2}\frac{F}{c^{3/2}} \quad (2)$$

where K_R is the crack resistance, F is the applied indentation load, E and H are the elastic modulus and the hardness of the test material, respectively, δ is a dimensionless constant dependent only on the indenter geometry and has an empirical value of 0.016±0.004 for Vickers indentation-induced crack systems.[27]

Eq. (2) is the basic equation used in the DI method to measure the R-curve. In general, the crack half-length, c, used to calculate K_R was taken as the average over the two orthogonal radial directions, i.e. $c=(c_1+c_2)/2$.[27] If the R-curve behavior is indeed a crack-location dependent phenomenon, however, such a treatment seems to be questioned. Eq. (2) was established based on a consideration that, in the as-indented state, the indentation-induced crack system would be subject to conditions of mechanical equilibrium stated as $K_r=K_R$, where K_r is the driving force provided by the residual stress resulting from the mismatch between the plastic zone beneath the indentation and the surrounding elastic matrix. If the crack resistance varies with crack location as well as crack length, one can expect that there is a possibility for the two cracks associated with the same indentation to encounter different local crack resistances due to the fact that the two crack tips are located in different sites. In fact, our exploratory experiments showed that there always exists a deviation, which may be significant for some indentations and slight for other indentations, between the measured c_1 and c_2 for a given indentation. Therefore, for the study on the crack-location dependence of the R-curve behavior, it seems to be more reasonable to calculate the crack resistance with Eq. (2) using c_1 and c_2, respectively, to yield two K_R data from one indentation. In the present study, we adopted this approach to calculate K_R and, consequently, a total of 60 K_R data were obtained for each employed load level.

4. Data analysis

The crack half-length, c, and corresponding K_R measured at each indentation load level are summarized in Table 1. In this table, the average value and the standard deviation of the measured crack resistance, K_R, were calculated using 60 data extracted with the method described in the preceding section. As can be seen, the average value of the crack resistance increases with increasing indentation load, indicating that the Al_2O_3–TiC composite examined in the present study possesses a significant R-curve behavior.

However, the large scatter in the measured K_R is also significant. At each load level, the coefficient of variation of K_R, i.e. the ratio of the standard deviation to the average value, is larger than 10%. There is reason to believe that the existence of the large scatter in K_R determined with the DI method is a universal phenomenon. The DI method has been widely employed by other authors to evaluate the R-curve behavior for other ceramics. The coefficient of variation of the measured K_R reported in the previous studies was usually large, typically around 10% (see for examples Table 2 in Ref. 18 and Table 3 in Ref. 28).

Fig. 3 shows, as examples, the histograms as well as the empirical probability density functions (PDFs) for the K_R-data measured at loads of 49 and 294 N, respectively. The empirical probability density curves shown in these plots were constructed by assuming that the data follow a Weibull distribution or a Gaussian distribution, respectively. The PDF for the Gaussian

Table 1
Summary of the Vickers indentation test results obtained in the present study

Indentation load, F(N)	Crack half-length, c (μm)			Crack resistance	Weibull analysis for K_R	
	Average	Minimum	Maximum	K_R (MPa·m$^{1/2}$)	m	K_0 (MPa·m$^{1/2}$)
49	88.7±10.6	73.4	118.4	5.0±0.8	7.22	5.4
98	135.3±12.5	112.8	168.4	5.3±0.7	9.23	5.6
196	209.6±15.3	181.6	246.8	5.5±0.6	11.52	5.7
294	267.1±20.5	239.5	323.2	5.7±0.6	11.35	6.0

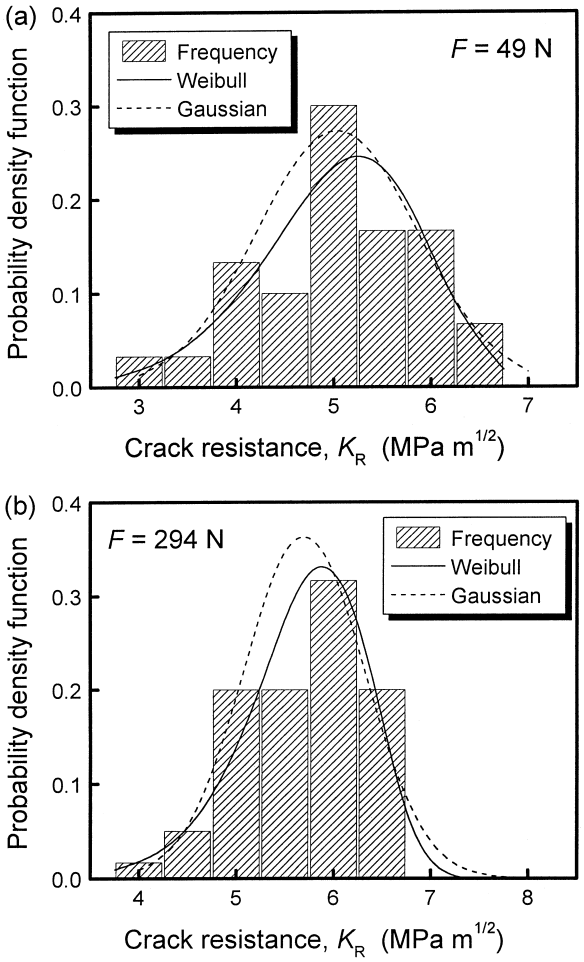

Fig. 3. Histogram and probability density functions plots for the K_R data measured at loads of 49 N (a) and 294 N (b).

distribution (as shown by the dashed line) is a bell-shaped curve, while the PDF for the Weibull distribution (as shown by the solid line) is skewed to the right. Noting the asymmetry in each of the histograms, one can conclude that the statistical properties of the measured K_R may not be described properly with the Gaussian distribution. Consequently, it may be insufficient to represent the measured K_R only with an average value and a standard deviation. Furthermore, From a viewpoint of statistics, such a large scatter would also make it insufficient to determine the crack resistance with a small number of measurements with the DI method.

As can be seen in Fig. 3, the Weibull distribution seems to be more suitable than the Gaussian distribution for representing the measured K_R data. This was further confirmed from the tests of Pearson χ^2 which were conducted with the data measured at each load level, respectively, according to the standard statistics theory. The χ^2 tests showed that, in each case, the assumption that the measured K_C data follow a Weibull distribution can be accepted at a confidence level higher than 95%.

The experimental data were analyzed with the conventional least-square (LS) method[29] to yield the Weibull parameters, knowledge of which would lead to complete characterization of the statistical properties of the measured K_R data. This was done by ordering the results measured at each load level from the lowest to the highest. The ith result in the set of 60 data was assigned a cumulative probability of occurrence, P_i, which was calculated with

$$P_i = \frac{i - 0.5}{60}. \tag{3}$$

The measured indentation toughness, $(K_R)_i$, and the cumulative probability, P_i, were then analyzed, by using a simple, least-square regression method, according to the alternative form of the well-known two-parameter Weibull distribution equation[29]

$$\ln \ln\left(\frac{1}{1-P}\right) = m \ln K_R - m \ln K_0 \tag{4}$$

where m and K_0 are the Weibull modulus and the scale parameter, respectively.

Fig. 4 shows the Weibull plots for the K_R data measured at each load level, respectively. In each case, a good linear relationship between ln ln $[1/(1-P)]$ and ln K_R was observed, implying that the experimental data can be well described with the Weibull distribution equation. The resultant Weibull parameters, m and K_0, for each data set of K_R are summarized in Table 1.

5. Discussion

Based on the discussion conducted in Sections 1 and 3, the large scatter in the measured K_R may be attributed to the statistical variation in the crack resistance brought about by the microstructure. To support this statement, the crack patterns made with a load of 294 N were examined using scanning electron microscopy and examples of crack–microstructure interactions are shown in Fig. 5. In Fig. 5(a), the crack was located mainly in the Al_2O_3 and interacted occasionally with small TiC particles. However, the crack shown in Fig. 5(b) encountered large TiC particles and deflected more clearly compared with that shown in Fig. 5(a). As mentioned above, the TiC particle size in the examined composite exhibits a somewhat large scatter. Consequently, one can expect that cracks located in different sites in the specimen surface would encounter different microstructural features and, as a result, the crack resistances for different cracks would be different. In other words, the crack resistance depends not only on the crack length but also on the crack location.

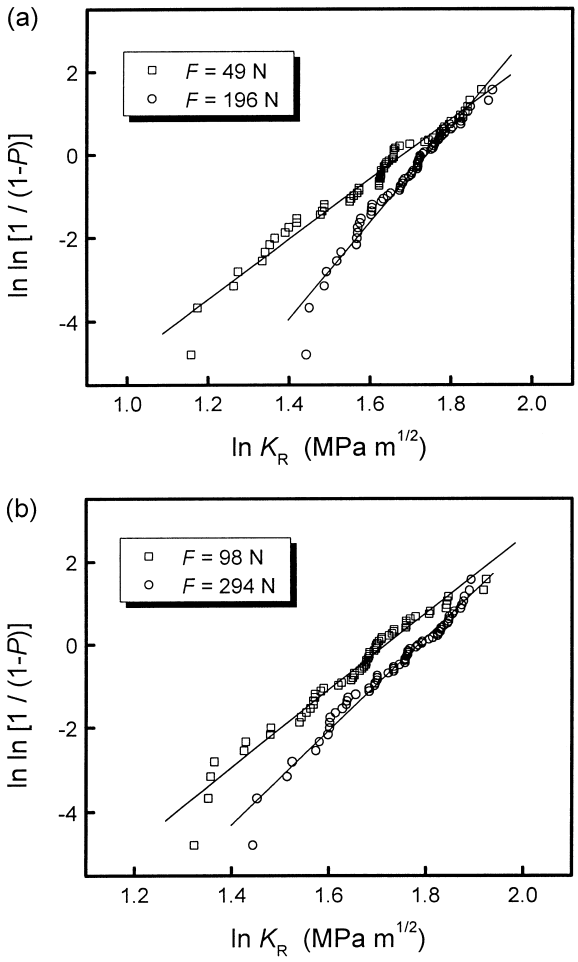

Fig. 4. Weibull plots for the K_R data measured at different load levels.

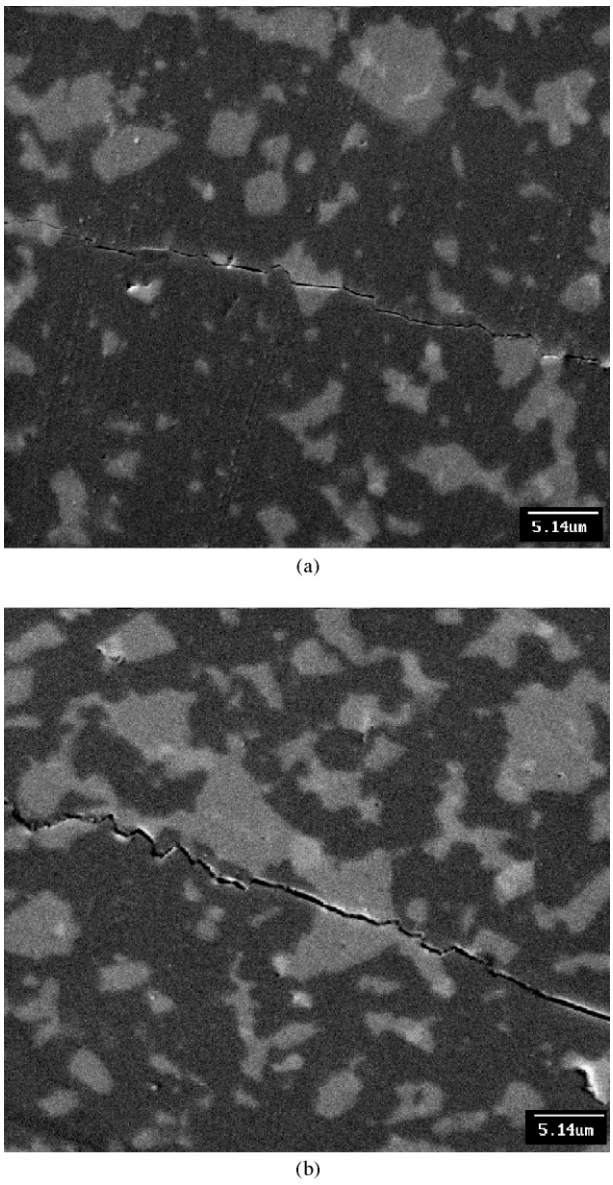

Fig. 5. SEM micrographs showing crack paths for different cracks in the specimen surface.

As shown in Table 1, the resultant Weibull modulus increases slightly with indentation load in the low load range ($F < 196$ N) and then tends to be invariable when the load increases further. This experimental finding seems to be a further support for the above discussion. Considering that, as the crack size increases, the probability for a crack to interact with the microstructural features having the largest resistance to fracture increases and, consequently, the dispersion of the measured crack resistance for cracks made at a given indentation load level but located at different sites would become small.

As mentioned in Section 1, the *R*-curve behavior of ceramics has been usually evaluated with indentation methods and deviations between the *R*-curves measured with different indentation methods have been frequently reported. Considering the existence of the crack-location dependence of the crack resistance, such deviations can be understood. The crack resistance measured with the DI method is only the local crack resistance which is strongly affected by the microstructural inhomogeneity. For the indentation-crack growth (ICG) method, the crack resistance is measured as a function of the crack length by propagating the crack under successively increasing applied load.[17] Since the crack direction or the cracking plane is predetermined, the measured *R*-curve reflects the crack-length dependence of the crack resistance for the given cross-section of the test specimen. However, the difference in the microstructural features in difference cross-sections of the test specimens would still make the measured *R*-curves different with each other and exhibit a significant crack-location dependence. In the indentation–strength (IS) method, the *R*-curve is evaluated by measuring the strength of the indented specimens.[15] The use of a single power law to describe the *R*-curve for a given material in this method ignores the differences between the details of the propagation procedure for different cracks. So the resultant *R*-curve cannot provide any useful information on the effect of

microstructural inhomogeneity on crack resistance. Therefore, the fact that different evaluation methods yield different *R*-curve behavior for a given material is not surprising.

It should be pointed out in closing that, from a practical viewpoint, the DI method seems to be the most suitable one to evaluate the *R*-curve behavior for ceramics, for it may provide a deeper knowledge of the microstructure-dependence of the crack resistance throughout the specimen surface. However, it is very important to conduct a large number of measurements at each load level to obtain a complete characterization of the statistical properties of the measured crack resistance.

References

1. Knehans, R. and Steinbrech, R., Memory effect of crack resistance during slow crack growth in notched Al_2O_3 bend specimens. *J. Mater. Sci. Lett.*, 1982, **1**, 327–329.
2. Majumber, B. S., Rosenfield, A. R. and Duckworth, W. H., Analysis of *R*-curve behavior of non-phase-transforming ceramics. *Engng Fract. Mech.*, 1988, **31**, 683–701.
3. Evans, A. G., Perspective on the development of high-toughness ceramics. *J. Am. Ceram. Soc.*, 1990, **73**, 187–206.
4. Becher, P. F., Microstructural design of toughened ceramics. *J. Am. Ceram. Soc.*, 1991, **74**, 255–269.
5. Steinbrech, R. W., Microstructural design of toughened ceramics. In *Fracture Mechanics of Ceramics*, Vol. 9, ed. R. C. Bradt, D. P. H. Hasselman, D. Munz, M. Sakai and V. Ya. Shevchenko. Plenum, New York, 1992, pp. 187–208.
6. Faber, K. T. and Evans, A. G., Crack deflection process: II, experiments. *Acta Metall.*, 1983, **31**, 577–584.
7. Evans, A. G. and Faber, K. T., Crack-growth resistance of microcracking brittle materials. *J. Am. Ceram. Soc.*, 1984, **67**, 255–260.
8. Marshall, D. B., Strength characteristics of transformation-toughening zirconia. *J. Am. Ceram. Soc.*, 1986, **69**, 173–180.
9. Heuer, A. H., Transformation toughening in ZrO_2-containing ceramics. *J. Am. Ceram. Soc.*, 1987, **70**, 689–698.
10. Swanson, P. L., Fairbanks, C. J., Lawn, B. R., Mai, Y. W. and Hockey, B. J., Crack-interface grain bridging as a fracture resistance mechanism in ceramics: I, experimental study on alumina. *J. Am. Ceram. Soc.*, 1987, **70**, 279–289.
11. Rodel, J., Kelly, J. F. and Lawn, B. R., In situ measurements of briding crack interfaces in the scanning electron microscopy. *J. Am. Ceram. Soc.*, 1990, **73**, 3313–3318.
12. Faber, K. T. and Evans, A. G., Crack deflection process: I, theory. *Acta Metall.*, 1983, **31**, 545–576.
13. Evans, A. G. and Cannon, R. M., Toughening of brittle solids by martensitic transformation. *Acta Metall.*, 1986, **34**, 761–800.
14. Mai, Y. W. and Lawn, B. R., Crack-interface grain bridging as a fracture resistance mechanism in ceramics: II, theoretical fracture mechanics model. *J. Am. Ceram. Soc.*, 1987, **70**, 289–294.
15. Krause, R. F., Rising fracture toughness from the bending strength of indented alumina beams. *J. Am. Ceram. Soc.*, 1988, **71**, 338–343.
16. Anderson, R. M. and Braun, L. M., Technique for the *R*-curve determination of Y-TZP using indentation-produced flaws. *J. Am. Ceram. Soc.*, 1990, **73**, 3059–3062.
17. Ramachandran, N. and Shetty, D. K., Rising crack-growth-resistance (*R*-curve) behavior of toughened alumina and silicon nitride. *J. Am. Ceram. Soc.*, 1991, **74**, 2634–2641.
18. Choi, S. R. and Salem, J. A., Crack-growth resistance of in situ-toughened silicon nitride. *J. Am. Ceram. Soc.*, 1994, **77**, 1042–1046.
19. Kim, Y. W., Mitomo, M. and Hirosaki, N., *R*-curve behavior of sintered silicon nitride. *J. Mater. Sci.*, 1995, **30**, 4043–4048.
20. Cook, S. G., King, J. E. and Little, J. A., Surface and subsurface Vickers indentation cracks in SiC, Si_3N_4, and sialon ceramics. *Mater. Sci. Technol.*, 1995, **11**, 1093–1098.
21. Alcala, J. and Anglada, M., Indentation precracking of Y-TZP: implications to *R*-curves and strength. *Mater. Sd. Engng*, 1998, **A245**, 267–276.
22. Steinbrech, R. W., Knehans, R. and Schaarwachter, W., Increase of crack resistance during slow crack growth in Al_2O_3 bend specimens. *J. Mater. Sci.*, 1983, **18**, 265–270.
23. Salem, J. A. and Shannon, J. L., Fracture toughness of Si_3N_4 measured with short bar chevron-notched beams. *J. Mater. Sci.*, 1987, **22**, 321–324.
24. Gong, J. and Guan, Z., Crack-location-dependent *R*-curve behavior in Si_3N_4. *J. Eur. Ceram. Soc.*, 2000, **20**, 1895–1900.
25. Marshall, D. B., Noma, T. and Evans, A. G., A simple method for determining elastic-modulus-to-hardness ratios using Knoop indentation measurements. *J. Am. Ceram. Soc.*, 1982, **65**, C175–Cl76.
26. Lawn, B. R., Evans, A. G. and Marshall, D. B., Elastic/plastic indentation damage in ceramics: the median/radial crack system. *J. Am. Ceram. Soc.*, 1980, **63**, 574–581.
27. Anstis, G. R., Chantikul, P., Lawn, B. R. and Marshall, D. B., A critical evaluation of indentation techniques for determining fracture toughness: I, direct crack measurements. *J. Am. Ceram. Soc.*, 1981, **64**, 533–538.
28. Franco, A., Robert, S. G. and Warren, P. D., Fracture toughness, surface flaw sizes and flaw densities in Al_2O_3. *Acta Mater.*, 1997, **45**, 1009–1015.
29. Quinn, G. D., Flexure strength of advanced structural ceramics: a round robin. *J. Am. Ceram. Soc.*, 1990, **73**, 2374–2384.